

Nonequilibrium Phase Transition and Self-Organized Criticality in a Sandpile Model with Stochastic Dynamics

S. Lübeck^{1*}, B. Tadić^{2†} and K. D. Usadel^{1◇}

¹*Theoretische Tieftemperaturphysik, Gerhard-Mercator-Universität Duisburg,*

Lotharstr. 1, 47048 Duisburg, Germany

²*Jožef Stefan Institute, University of Ljubljana,*

P.O. Box 100, 61111-Ljubljana, Slovenia

(14. September 1995)

We introduce and study numerically a directed two-dimensional sandpile automaton with probabilistic toppling (probability parameter p) which provides a good laboratory to study both self-organized criticality and the far-from-equilibrium phase transition. In the limit $p = 1$ our model reduces to the critical height model in which the self-organized critical behavior was found by exact solution [D. Dhar and R. Ramaswamy, Phys. Rev. Lett. **63**, 1659 (1989)]. For $0 < p < 1$ metastable columns of sand may be formed, which are relaxed when one of the local slopes exceeds a critical value σ_c . By varying the probability of toppling p we find that a continuous phase transition occurs at the critical probability p_c , at which the steady states with zero average slope (above p_c) are replaced by states characterized by a finite average slope (below p_c). We study this phase transition in detail by introducing an appropriate order parameter and the order-parameter susceptibility χ . In a certain range of $p < 1$ we find the self-organized critical behavior which is characterized by nonuniversal p -dependent scaling exponents for the probability distributions of size and length of avalanches. We also calculate the anisotropy exponent ζ and the fractal dimension d_f of relaxation clusters in the entire range of values of the toppling parameter p . We show that the relaxation clusters in our model are anisotropic and can be described as fractals for values of p above the transition point. Below the transition they are isotropic and compact.

05.40.+j

I. INTRODUCTION

The term "self-organized criticality" (SOC) [1] refers to certain driven dissipative systems which organize themselves into a steady state far away from equilibrium. The critical steady state appears as an attractor of the dynamics, and thus no fine tuning of an external parameter is necessary to achieve criticality. The major aspect of the dynamics of SOC systems is the "separation of time scales", i.e. the system relaxes infinitely fast compared to the time between two successive perturbations. From this point of view the relaxation processes may be considered as consisting of a series of discrete events (avalanches) and one investigates the probability distribution of their spatial properties, for instance the size of an avalanche. The self-organized critical state is characterized by a power-law behavior of these probability distributions. For detailed discussions of the definition of SOC we refer to [2,3].

Sandpile automata [1,4,5] are well known prototype models exhibiting SOC. By adding a particle from the outside, a sandpile is perturbed and the perturbation may lead to instabilities at neighboring sites if the local height of sand exceeds a critical value h_c (critical height model (CHM) [1,4]), or if the local slopes exceed a critical value σ_c (critical slope model (CSM) [5-7]). The steady state of the system in the case of the CHM is accompanied with a state of a zero average slope. A finite average slope characterizes a CSM.

In Section II we introduce a two dimensional directed sandpile model with stochastic dynamics, in which the updating rules may be tuned continuously by varying a parameter p , representing probability of toppling, between CHM (for $p = 1$) and CSM (for $p = 0$) [8]. Our numerical results for $p < 1$ show that a nonequilibrium phase transition takes place at the critical value p_c , which is characterized by a continuous appearance of a non zero average slope below the critical point. In order to characterize this phase transition quantitatively, we introduce an order parameter $\langle \sigma \rangle$, representing net average slope. Results obtained from numerical simulations of the order parameter $\langle \sigma \rangle$, as well as the order parameter susceptibility and the penetration depth of the slope will be given in Section III.

We also study fractal properties of the avalanches by calculating their fractal dimension in the entire range of values of the parameter p (Section IV). Our results suggest that for values of p above the transition point the avalanches can be described as self-affine fractals, i.e. the shape of the avalanches exhibits an anisotropic behavior. Below the transition point both properties, the fractality and anisotropy of the relaxation clusters, are lost.

In Section V we present a detailed analysis of the probability distributions of the avalanches and address the question whether the model exhibits SOC for $p < 1$. A finite size scaling analysis of the probability distributions and a check of certain scaling equations yielded that the

model displays SOC for certain values of $p < 1$.

II. MODEL

We consider a two-dimensional sandpile model on a square lattice of size $L \times L$ and integer variables $h(i, j)$ representing the local height. We assume a directed dynamics, i.e. particles are restricted to flow in the downward direction (increasing i). According to the widespread 'sandpile language', the first row ($i = 1$) and the last row ($i = L$) represent the top and the bottom of the pile, respectively. To minimize the influence of the horizontal boundaries we limit our investigations to periodic boundary conditions in this horizontal direction (j -direction). Any site of the lattice has two downward and two upward next neighbours, namely $h(i+1, j_{\pm})$ and $h(i-1, j_{\pm})$ with $j_{\pm} = j \pm \frac{1}{2}(1 \pm (-1)^i)$.

We perturb the system by adding particles at a random place on the top of the pile according to

$$h(1, j) \mapsto h(1, j) + 1, \quad \text{with random } j. \quad (1)$$

A site is called unstable if the height $h(i, j)$ or at least one of the two slopes

$$\sigma(i, j_{\pm}) = h(i, j) - h(i+1, j_{\pm}) \quad (2)$$

exceeds its respective critical value, i.e. if $h(i, j) \geq h_c$ or $\sigma(i, j_{\pm}) \geq \sigma_c$.

If both slopes are critical one particle after another drops alternatively to the next downward neighbours until both slopes become subcritical. In the case that one slope exceeds σ_c particles drop to the corresponding downward neighbour.

In contrast to the critical slope, the critical height condition has a stochastic character. If the local height exceeds the critical value h_c toppling occurs only with the probability p , and then two particles drop to the two downward neighbours.

Because each relaxing cell changes the heights or slopes of its four neighbouring sites, the stability conditions are applied at these four activated sites in the next updating step. Toppling may take place after adding a particle on the first row. We apply the slope and the height stability condition simultaneously for all activated sites. An avalanche stops if all activated sites are stable. Then we start again according to Eq. (1).

It should be emphasized that, in addition to the instability criteria, a site is considered as potentially unstable *only* when a particle drops at or near the site. Owing to the probabilistic character of the critical height toppling rule, locally heights could remain above critical after one relaxation event. In this respect, the present model for $0 < p < 1$ is different from already known critical height [1,4,5] and critical slope [5,6] models.

One can interpret the parameter $1 - p$ as being due to static friction between the sand grains, which prevents

toppling even if the height exceeds the critical value. In the case $p = 1$, our model is identical to the model of Dhar and Ramaswamy [4], which exhibits a robust SOC behavior. In the limit $p = 0$, our directed rules lead to a steady state where all slopes are equal, i.e. $\sigma(i, j_{\pm}) = \sigma_c - 1$. Thus, if a particle is added at the first row it performs a directed random walk downward the pile until it reaches the boundary and drops out of the system — no SOC can occur in this limit.

We fix the critical height h_c and the critical slope σ_c and restrict ourselves to $h_c = 2$ and $\sigma_c = 8$, although it should be emphasized that the results depend on the choice of these parameters.

The behavior of our model is characterized by anisotropy effects caused by the preferred direction of the assumed dynamics. This anisotropy may influence for instance the fractal properties of the avalanches. If a measured quantity depends on the direction we introduce in these cases two different values which describe the behavior in parallel and perpendicular direction respectively, e.g. the fractal dimensions d_{\parallel} and d_{\perp} . The parallel direction corresponds to the preferred direction of the dynamics (increasing i).

III. NONEQUILIBRIUM PHASE TRANSITION

In this section we consider the general behavior of the system, i.e. how the transition from the CHM to the CSM takes place. As mentioned above a CHM is characterized by a zero average slope in contrast to a CSM where the steady state displays a non zero average slope. In order to describe this transition quantitatively, we introduce as an order parameter the mean slope of the system [8]

$$\langle \sigma \rangle = \frac{1}{L_{\parallel} L_{\perp}} \sum_{i,j} \langle \sigma_{ij} \rangle \quad (3)$$

where $\langle \dots \rangle$ stands for the average over total number of events, and σ_{ij} is the local slope at site (i, j) which is defined as

$$\sigma_{ij} = \frac{1}{2}(2h_{i,j} - h_{i+1,j+} - h_{i+1,j-}). \quad (4)$$

The summation in Eq. (3) runs from $j = 1, 2, 3, \dots, L$ in perpendicular direction, and from $i = 21, 22, \dots, L - 20$ in parallel direction, in order to suppress the boundary effects from the first and last row of the system. Of course the obtained results are independent of the value of the cut off length, provided that it is large enough. To normalize the order parameter one has to choose $L_{\parallel} = L - 40$ and $L_{\perp} = L$. The nature of the transition as well as the transition point p_c should be determined from the p -dependence of the average slope Eq. (3) in the vicinity of p_c .

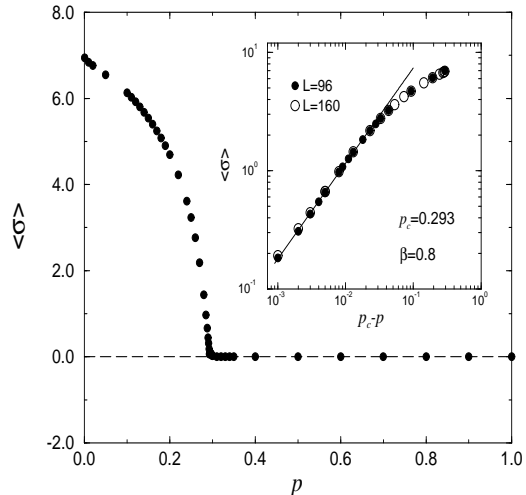


FIG. 1. Average slope of the pile $\langle \sigma \rangle$ plotted vs. probability p . The solid line inside the inset corresponds to a fit according to Eq. 3.

In Fig. 1 we show the results of numerical simulations of the order parameter defined in Eq. (3). The order parameter vanishes at the transition point as, i.e.,

$$\langle \sigma \rangle \sim (p_c - p)^{\beta}, \quad (5)$$

as one can see from the inset of Fig. 1. We determine the transition point $p_c = 0.293 \pm 0.002$ and the exponent $\beta = 0.8 \pm 0.05$ for automaton sizes $L = 64, 96, 128, 160, 192$.

We next analyze the fluctuation of the order parameter. An ordering susceptibility can be defined as [9]

$$\chi = L_{\parallel} L_{\perp} (\langle \sigma^2 \rangle - \langle \sigma \rangle^2). \quad (6)$$

Unfortunately the average slope has as a self-averaging character in the critical height regime, that means χ vanishes for $L \rightarrow \infty$ due to a cancellation of the correlations $\langle \sigma_{ij} \sigma_{kl} \rangle$ in the interior of the pile. Consequently the susceptibility depends only on the boundary term and is of relative magnitude $\sim L_{\parallel}^{-1}$. In the case $p = 1$ the order parameter susceptibility can be calculated exactly and is given by

$$\chi = \frac{1}{2L_{\parallel}}. \quad (7)$$

In Fig. 2 we display the susceptibility χ for varying p and four different automata sizes. For all considered automata sizes χ is sharply peaked at the transition point $p_c = 0.293$.

In the inset of Fig. 2 we plot $\chi \cdot L_{\parallel}$ vs. p . All different curves collapse, except of the values which are close to the transition point. The susceptibility scales as

$$\chi \sim L_{\parallel}^{-1} (p - p_c)^{-\gamma} \quad (8)$$

with $\gamma = 0.98 \pm 0.05$. One can see from Fig. 2 that this power law behavior of χ holds away from p_c up to a

certain cut off value which tends to p_c if $L \rightarrow \infty$. Due to this L -dependence the order parameter susceptibility tends to zero with increasing L for $p > p_c$.

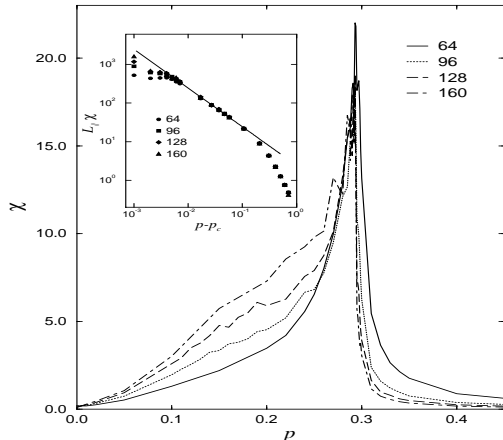


FIG. 2. The p -dependence of the order parameter susceptibility for different system sizes L . The inset displays the scaling behavior of the height regime. The solid line corresponds to a power law with exponent $\gamma = 0.98$.

Below the critical point our data suggest that the susceptibility displays a complicated scaling behavior (see Fig. 2). It is still an open question whether χ diverges with increasing systems size L or converges to a finite i.e. L -independent value. To address this question one has to simulate extremely large systems which is beyond our present computer capacity.

In order to break off the self-averaging character of the average slopes we defined a nonlinear-susceptibility

$$\chi_{nl} = L_{\parallel} L_{\perp} (\langle \sigma_{nl}^2 \rangle - \langle \sigma_{nl} \rangle^2) \quad (9)$$

with

$$\sigma_{nl} = \frac{1}{L_{\parallel} L_{\perp}} \sum_{i,j} \sigma_{ij}^2. \quad (10)$$

We found that χ_{nl} shows a cusp at p_c , i.e. the nonlinear-susceptibility is independent of L in both regimes (not shown). This behavior is consistent with the exact value for $p = 1$:

$$\chi_{nl} = \frac{9}{64} + \mathcal{O}(L^{-1}). \quad (11)$$

The non-diverging behavior of the susceptibilities indicate that the non equilibrium phase transition is not characterized by a diverging correlation length. Thus we address the question how the finite slope occurs by approaching the transition point. In Fig. 3 we display the average height profile $\langle h \rangle(i)$ of the pile for certain values

of p . For $p < 1$ a finite slope occurs at the boundaries and the pile grows up from the bottom of the pile. The slopes penetrate the hole system from the edge of the automaton.

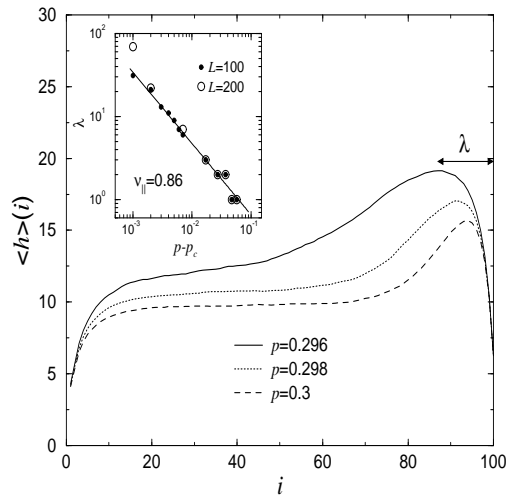


FIG. 3. The average height profile $\langle h(i) \rangle$ along the parallel direction. The penetration depth λ is determined as the distance from the maximum height to the right boundary of the system. The inset displays the p -dependence of λ .

We determine the penetration depth λ of the slopes by measuring the distance of the profile maximum from the right boundary (see Fig. 3). The obtained results are plotted in the inset of Fig. 3 for automaton sizes $L = 100, 200$. Close to the transition point the penetration depth obeys a power law behavior like

$$\lambda \sim (p - p_c)^{-\nu_{\parallel}}. \quad (12)$$

Our numerical analysis yielded $\nu_{\parallel} = 0.86 \pm 0.06$.

IV. FRACTAL PROPERTIES OF THE AVALANCHES

In this section we consider the scaling properties of the avalanches. We define the size s of the avalanches as the number of toppled sites in one event. The length of an avalanche is defined as the distance from the first row to the toppled site with maximal value of the index i . Note that this length is by definition parallel to the preferred direction, and will be denoted as l_{\parallel} . We introduce the average width l_{\perp} of an avalanche via

$$l_{\perp} = \left(l_{\parallel}^{-1} \sum_{i=1}^{l_{\parallel}} l_{\perp}(i)^q \right)^{\frac{1}{q}}, \quad (13)$$

where $l_{\perp}(i)$ is the width of an avalanche in the i th row. Since there is some arbitrariness in the definition of l_{\perp}

we both tried $q = 1$ and $q = 2$ with the result that the scaling properties of the width are practically the same in both cases. For the sake of simplicity we present in this paper only the results for $q = 2$. We assume that the size of avalanches is scale invariant both with the length and width. In order to take the anisotropy of avalanches into account, we introduce two different scaling exponents d_{\parallel} and d_{\perp} , corresponding to different directions of scaling l_{\parallel} and l_{\perp} , respectively [10,11]. We assume that the average size $\langle s \rangle$ of all avalanches of length l_{\parallel} and of width l_{\perp} , respectively, scales as

$$\langle s \rangle_{l_{\parallel}} \sim l_{\parallel}^{d_{\parallel}} \quad \text{and} \quad \langle s \rangle_{l_{\perp}} \sim l_{\perp}^{d_{\perp}}. \quad (14)$$

If both scaling relations are valid the width scales with the length like

$$l_{\perp} \sim l_{\parallel}^{\zeta}, \quad \text{with} \quad \zeta = \frac{d_{\parallel}}{d_{\perp}}. \quad (15)$$

where the exponent ζ describes the anisotropic behavior of the avalanches. Since there are only two independent exponents we measured d_{\parallel} and ζ according to Eq. (13)-Eq. (15).

We find that with decreasing p the parallel fractal dimension d_{\parallel} increases from the exactly known value $d_{\parallel} = \frac{3}{2}$ in the limit $p = 1$ to two at the transition point. In the critical slope regime d_{\parallel} remains constant and $d_{\parallel} = 2$ [8].

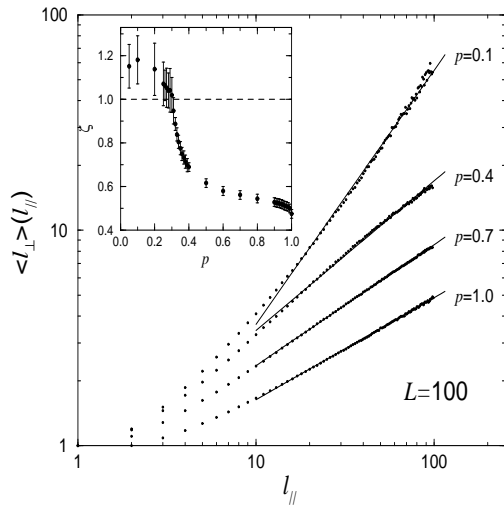


FIG. 4. Double logarithmic plot of the average width vs. length for various values of p as indicated. All curves obey a power law behavior (solid lines) with different accuracy. The inset displays the p -dependence of the anisotropic exponent ζ obtained from the fits according to Eq. 15.

Fig. 4 shows how the width depends on the length for different values of p . In all cases we found that Eq. (15) is valid and extracted values of the anisotropy exponent

ζ (see inset to Fig. 4). With decreasing p the anisotropy exponent ζ increases from $\zeta = \frac{1}{2}$ at $p = 1$ and reaches its maximum value $\zeta \simeq 1$ for $p \leq p_c$. We expect that this expression is exactly given by $\zeta = 1$ and that the observed deviations in the critical slope regime are caused by finite size effects. The origin of the huge error bars for $p < p_c$ is a finite curvature of the corresponding curves in the log-log plots. These curvatures would be reduced by studying larger systems leading eventually to the result $\zeta = 1$ with higher accuracy. Thus, the critical height regime is characterized by an anisotropic shape of the avalanches ($\zeta < 1$). This behavior changes to an isotropic shape ($\zeta = 1$) on approaching the transition point. Due to the dependence of the scaling factors on the directions the avalanches can be regarded as an example of self-affine fractals. In analogy to self-similar fractals, it is possible to describe self-affine fractals by single exponent d_f , given by [11]

$$d_f = 2 \frac{d_{\parallel}}{\zeta + 1}. \quad (16)$$

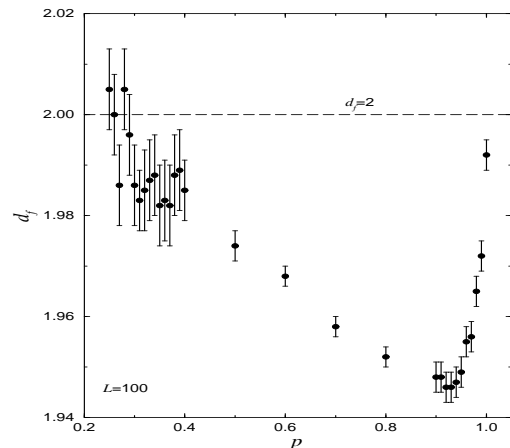


FIG. 5. Fractal dimension d_f of the avalanches for various values of p .

In Fig. 5 we show the results for the fractal dimension d_f versus p in the critical height regime. As seen from Fig. 5, the relaxation clusters exhibit a fractal behavior ($d_f < 2$) in the critical height regime $p > p_c$, with exception of the case $p = 1$. Although the deviation from $d_f = 2$ is very small they cannot be explained by statistical fluctuations due to the size of the error bars and the systematic way of the deviations from 2. Below the transition point, i.e., for $p < p_c$, the fractal dimension $d_f = 2$, corresponding to compact clusters.

One can easily explain this behavior by considering the shapes of the avalanches (see Fig. 4 in [8]). In the pure critical height model ($p = 1$) the avalanches are compact, i.e. no holes can occur in this limit. With decreasing p

some supercritical sites may remain in the interior of the avalanche due to the stochastic character of the dynamics, leading to holes and branching processes. This results in a fractal character of the avalanches. By approaching the transition point p_c this structure of the avalanches is lost. In this region the dynamics is more and more characterized by toppling processes due to the critical slope condition. The slope between a toppled site and its two backward neighbours may exceed the critical value and toppling occurs again. Owing to this multiple topplings the probability to find holes inside an avalanche decreases with decreasing p and eventually vanishes at p_c . At the same time branching of the relaxation clusters become more rare.

In this way, we may conclude that the phase transition from the critical height to the critical slope regime is accompanied by continuous change from fractal avalanches with an anisotropic shape above p_c to compact and isotropic avalanches below p_c .

V. AVALANCHES DISTRIBUTIONS

In this section we examine how the SOC behavior of the Dhar model vanishes with decreasing p . In the critical state, due to the absence of a characteristic length scale, the probability $P(l_{\parallel})$ for an avalanche longer than a certain length l_{\parallel} obeys a power-law, i.e.,

$$P(l_{\parallel}) \sim l_{\parallel}^{-\kappa}. \quad (17)$$

Similarly, the probability distribution of an avalanche size larger than s exhibits a power law with another exponent via

$$P(s) \sim s^{-\tau}, \quad (18)$$

where s is the number of different sites that relaxed in one event. Multiply relaxed sites are counted only once in this distribution. Double logarithmic plots of the distributions $P(l_{\parallel})$ and $P(s)$ for various values of the parameter p and $L = 200$ are shown in Fig. 6 and Fig. 7.

TABLE I. The exponents for different values of toppling parameter p . Due to a lack of a power law behavior of the corresponding quantities the exponents τ, κ and θ are not defined for $p < 0.5$.

p	d_{\parallel}	ζ	z	τ	κ	θ
1.0	1.47	0.48	1.00	0.34	0.50	0.51
0.9	1.49	0.53	1.03	0.46	0.68	0.61
0.8	1.51	0.55	1.06	0.47	0.72	0.65
0.7	1.53	0.56	1.10	0.49	0.75	0.67
0.6	1.56	0.58	1.15	0.53	0.79	0.69
0.5	1.60	0.62	1.21	0.58	0.86	0.75
0.4	1.68	0.69	1.33	-	-	-
0.3	2.01	1.02	1.70	-	-	-
0.2	2.11	1.14	1.77	-	-	-
0.1	2.08	1.18	1.76	-	-	-

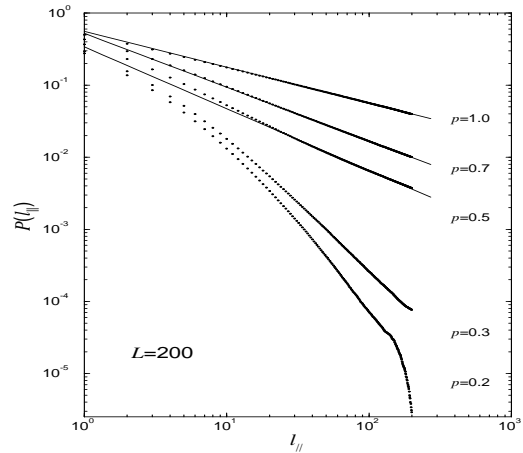


FIG. 6. Double logarithmic plot of the probability distribution $P(l_{\parallel})$ of avalanches of length l_{\parallel} for various values of p as indicated. The solid lines correspond to power laws.

One can see from Fig. 6 that the probability distribution $P(l_{\parallel})$ displays no cut-off in the critical height regime. For $p < p_c$ a sharp cut-off length occurs in the distribution $P(l_{\parallel})$. The dynamics is now dominated by the toppling processes due to the critical slope condition and thus the edge of the system ($i = L$) influences the topplings at a certain number of rows close to the edge. This behavior is typical for critical slope models.

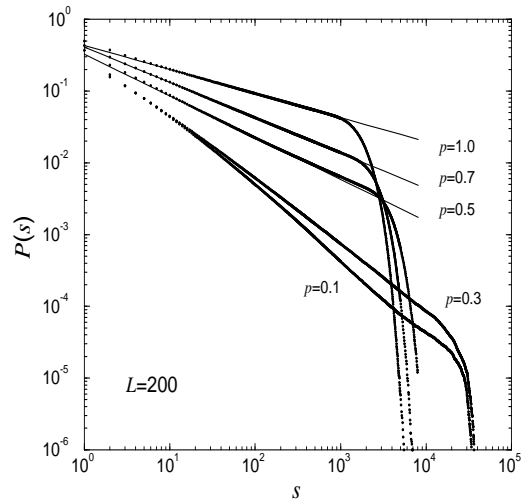


FIG. 7. Double logarithmic plot of the probability distribution $P(s)$ of avalanches of size s for various values of p as indicated. The solid lines correspond to power laws.

Power law behavior according to Eq. 17 and Eq. 18 occurs only in the critical height regime. The critical

exponents κ and τ are determined by the slopes of the linear sections of these curves for $p \geq 0.5$. For lower values of p we found a finite curvature in the log-log plots of the distributions, indicating that the power-law behavior is lost for a range of values of p preceding the transition point p_c . The obtained values of the exponents for certain values of p are shown in Fig. 8 and are listed in Table I. In the limit $p = 1$ the numerical values of the exponents coincide with the exact values [4] $\kappa = \frac{1}{2}$ and $\tau = \frac{1}{3}$.

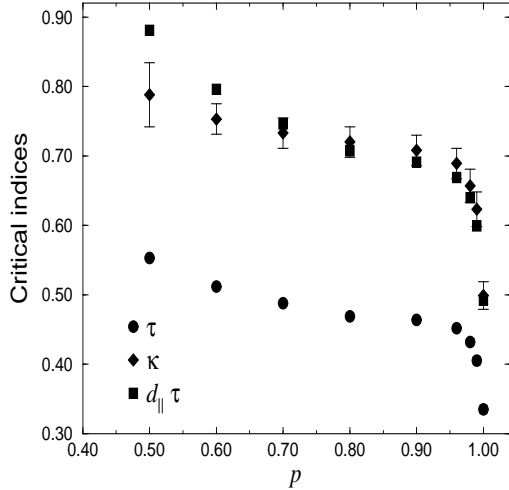


FIG. 8. Critical exponents κ and τ determined from the power law fits according to Eq. 17 and Eq. 18. In the case of the exponent τ the error bars are smaller than the symbols. The scaling equation Eq. 24 holds for $p > 0.6$.

We should emphasize that the above analysis is not a sufficient evidence that the model exhibits SOC for $p \geq 0.5$. To improve the accuracy of the results we analyse the effects due to the finite size of the systems by using simple finite-size scaling [6]:

$$P(s, L) = L^{-\beta_s} g(s L^{-\nu_s}). \quad (19)$$

In order that Eq. (18) is recovered for large L the universal function $g(x)$ must obey a power-law behavior for $x \rightarrow 0$ and the three exponents β_s , ν_s and τ fulfill the relation

$$\beta_s = \nu_s \tau. \quad (20)$$

The scaling exponent ν_s can be derived from the fractal dimension $d_{||}$: For each value of p we find a cut-off of the distribution taking place at a size s_{max} which depends on L . If finite-size scaling works all distributions $P(s, L)$, including their cut-offs, have to collapse, i.e. the argument of the universal function g has to be constant:

$$s_{max} L^{-\nu_s} = \text{const.} \quad (21)$$

On the other hand we know from Eq. (14) that $\langle s \rangle(l_{||})$ scales with the length $l_{||}$. Thus $\langle s_{max} \rangle$ scales with L in the same way and both exponents are identical. In this way we have calculated the scaling exponents

$$\beta_s = d_{||} \tau \quad \text{and} \quad \nu_s = d_{||} \quad (22)$$

from the measured exponents $d_{||}$ and τ .

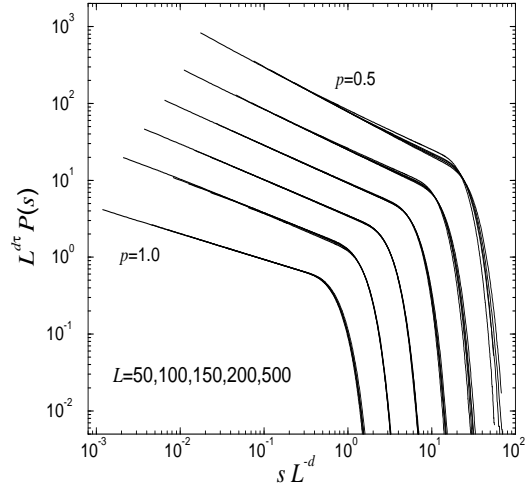


FIG. 9. Finite size scaling analysis of the avalanche size distribution $P(s)$ for $p = 1.0, 0.9, 0.8, 0.7, 0.6, 0.5$ and five different system sizes L . The curves corresponding to $p < 1$ are shifted in the upper right direction. The finite size scaling ansatz works quite well for $p > 0.6$.

In Fig. 9 we show the results of the scaling plot for $p \geq 0.5$ and five different automata sizes. Finite-size scaling works well for $p \geq 0.7$. In the case of $p \leq 0.6$ the deviations grow, i.e., the different curves do not completely collapse.

In the following we will prove a scaling relation among the exponents τ , κ and $d_{||}$, indicating that the exponents of the distributions $P(s)$ and $P(l_{||})$ are not independent. The relation

$$p(l_{||}) dl_{||} \sim p(l_{||}) \frac{dl_{||}}{ds} ds \sim p(s) ds \quad (23)$$

and Eq. (14) lead to the scaling relation

$$\kappa = d_{||} \tau. \quad (24)$$

Here $p(l_{||})$ and $p(s)$ represent the probability density of an avalanche of length $l_{||}$ and size s , i.e. they obey the power-laws $p(l_{||}) \sim l_{||}^{-\kappa-1}$ and $p(s) \sim s^{-\tau-1}$, with κ and τ defined in (17) and (18), respectively.

In Fig. 8 the product $d_{||} \tau$ is also shown and compared with the values of the exponent κ for various values of p . We conclude that the scaling relation (24) holds for

$p \geq 0.7$. These results confirm the finite-size scaling analysis and suggest that criticality is lost at a certain point between $p = 0.6$ and $p = 0.7$. We expect that preceding the transition point p_c the occurrence of toppling processes due to the critical slope condition increases and results in a loss of criticality which is connected to the pure critical height behavior.

We have also investigated the avalanches durations t and found that the average duration scales with the length $l_{||}$ according to

$$\langle t \rangle_{l_{||}} \sim l_{||}^z. \quad (25)$$

Analogous to the size s the probability distribution of the duration obeys a power-law behavior

$$P(t) \sim t^{-\theta} \quad (26)$$

for $p \geq 0.7$. In the same area of p finite-size scaling works quite well and the corresponding scaling relation $\kappa = z\theta$ is fulfilled. The obtained values of the exponents θ and z are listed in Table I. These measurements confirm our previous conclusion that the system exhibits SOC for $p \geq 0.7$ and not in the whole critical height regime.

VI. CONCLUSIONS

We have studied numerically a sandpile model with stochastic dynamics which exhibits a nonequilibrium phase transition as the parameter p (representing static friction) is varied. The probability parameter allows us to tune the dynamics from a critical height to a critical slope behavior. The average net slope $\langle \sigma \rangle$ plays the role of the order parameter and obeys a power law dependence in $p_c - p$. In contrast to the diverging penetration depth both the linear and nonlinear susceptibility shows no singular behavior by approaching the transition point p_c .

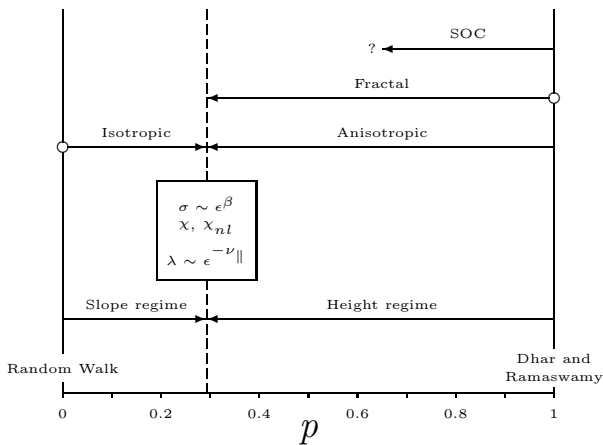


FIG. 10. Phase diagram of the model which illustrates the major properties of the investigated system. The order parameter σ and the penetration depth λ depend on $\epsilon = |p - p_c|$.

We found that the nonequilibrium phase transition is accompanied by a transition from an anisotropic to an isotropic behavior of the avalanches. Fractality occurs only in the case of the anisotropic shape of the avalanches.

Finite size scaling analysis works for the probability distributions of the avalanches and scaling relations hold for $p \geq 0.7$ indicating that the system exhibits SOC in this region. The corresponding exponents have a nonuniversal i.e. p -dependent behavior.

Due to long computation time, we did not simulate lattices larger than $L = 500$ in order to check if the power-law behavior is still maintained for values of $p < 0.6$. The problem of disappearance of the SOC on approaching the nonequilibrium phase transition remains for future study.

A complete illustration of the behavior of our sandpile model is depicted in Fig. 10.

ACKNOWLEDGMENTS

This work was supported by the Bundesministerium für Bildung, Wissenschaft, Forschung und Technologie, by the Deutsche Forschungsgemeinschaft through Sonderforschungsbereich 166, Germany, and by the Ministry of Science and Technology of the Republic of Slovenia.

* E-mail: sven@hal6000.thp.uni-duisburg.de

† E-mail: Bosiljka.Tadic@ijs.si

◇ E-mail: usadel@hal6000.thp.uni-duisburg.de

- [1] P. Bak, C. Tang and K. Wiesenfeld, Phys. Rev. Lett. **59**, 381 (1987).
P. Bak, C. Tang and K. Wiesenfeld, Phys. Rev. A **38**, 364 (1988).
- [2] G. Grinstein, in *Scale Invariance, Interfaces and Non-Equilibrium Dynamics*, edited by A. McKane *et al.*, NATO ASI Series B: Physics Vol. 344, Plenum Press (1995).
- [3] H. Flyvbjerg, in *Scale Invariance, Interfaces and Non-Equilibrium Dynamics*, edited by A. McKane *et al.*, NATO ASI Series B: Physics Vol. 344, Plenum Press (1995).
- [4] D. Dhar and R. Ramaswamy, Phys. Rev. Lett. **63**, 1659 (1989).
- [5] S. S. Manna, Physica A **179**, 249 (1991).
- [6] L. P. Kadanoff, S. R. Nagel, L. Wu and S. M. Zhou, Phys. Rev. A **39**, 6524 (1989).
- [7] S. Lübeck, K. D. Usadel, Fractals **1**, 1030 (1993).
- [8] S. Lübeck, B. Tadić and K. D. Usadel, in *Fractal Reviews in the Natural and Applied Sciences*, Proceedings of the Fractal conference in Marseille Feb. 1995, edited by M. M. Novak, Chapman & Hall (1995).
- [9] K. Binder and J.-S. Wang, J. Stat. Phys. **55**, 87 (1989).
- [10] W. Kinzel, Ann. Israel Phys. Soc., **5**, 425 (1983).
- [11] C. Kaiser and L. Turban, J. Phys. A: Math. Gen. **27**, L579 (1994).